13th World Conference on Earthquake Engineering
Vancouver, B.C., Canada
August 1-6, 2004
Paper No. 1267

A METHOD FOR NONLINEAR DYNAMIC RESPONSE ANALYSIS OF STRUCTURE CONSIDERING SOIL STRUCTURE INTERACTION

Hiroo SHIOJIRI[1], Makoto IROBE[2], Tomoyasu TAGUTI[3], Kenji GOTO[4] and Ablikim ABUDULA[5]

SUMMARY

A method for soil-structure interaction analysis considering non-linearity in the vast extent of foundation soil is proposed. Semi-infinite domain is mapped into finite domain. The resulting equations are solved with the two-step Lax-Wendoroff schemes. Non-linearity can be taken into account in the entire semi-infinite domain. The dynamic responses of soil-structure system are computed with small and extensive mesh models, and good agreements are obtained between the results of two models. It is shown that the dynamic response analysis of dam-reservoir-foundation system considering crack generation is effectively conducted by combining FEM with the proposed method.

INTRODUCTION

During severe earthquakes, nonlinear response of soil is observed in the extensive area. In the soil-structure interaction analysis, therefore, non-linearity in the response should be taken into account not only for the structure and soil near the structures but also for far field. There are two methods to deal with nonlinear soil structure interaction problems [1]. One is the direct method in which soil is modeled up to an artificial boundary. Since the boundary simulates the infinite extent of soil only approximately, the boundary should not be placed near the structure, leading to large degrees of freedoms. The other method is sub-structure method. In the substructure method, structure and near by soil with irregular geometry, material heterogeneity, and nonlinear behaviors are located in one substructure, and unbounded soil with regular geometry and linear material properties is analyzed in other substructure. In that case, non-linearity should be restricted near the structure. Here, a method for treating non-linearity in the vast extent of foundation soil is proposed. A special finite difference method is developed for nonlinear dynamic response analysis of semi-infinite foundation soil. At first, semi-infinite domain is mapped into finite domain using special mapping. Then, the resulting equations are solved with the two-step Lax-Wendoroff schemes on a uniform mesh of finite differences. Material non-linearity can be taken into account in the

[1] Prof., Nihon University, Email: shiojiri@civil.cst.nihon-u.ac.jp
[2] Prof., Nihon University
[3] Prof., Konan University
[4] M. Eng., Nihon University
[5] Dr. Eng., Nihon University

entire semi-infinite domain. This is the extension of the method, which mapping infinite domain, into finite domain described in [2][3][4], to nonlinear problem.

Methods

Shrinking mapping for hyperbolic problems

For $l > 0$, $L > l$, and $p > 0$, a non-negative, smooth function, $a(\xi)$, $\xi \in J = (-L, L)$ is taken, which satisfies:

$$a(\xi) = 1 \; for \; \xi \in I_\xi, \; I_\xi = \{\xi \mid \; |\xi| \le l\} \tag{1}$$

$$0 < a(\xi) < 1 \; for \; \xi \in J', \; J' = \{\xi \mid l < |\xi| < L\} \tag{2}$$

$$a(\xi) = 0(L - |\xi|)^{1+p} \text{ in } the \; neighbourhood \; of \; |\xi| = L \tag{3}$$

and a nonlinear mapping, G: $\xi \to x = \int_0^\xi d_T / a(_T)$ is defined. The mapping, G, maps J to $R^1 = (-\infty, \infty)$, one-to-one and onto such that it maps I_ξ to $I_x = \{x \mid \; |x| \le l\}$ isometrically, and J' (finite interval) to an infinite interval, $R' = \{x \mid l < |x| < \infty\}$; the latter can be stated that J' expands to R' by G, or alternatively, R' shrinks to J' by the inverse mapping, $\xi = G^{-1}[x]$ (Shrinking mapping). This mapping. $x = G[\xi]$ is used for the transformation of the coordinate variables 'shrink Consider the following first-order, scalar hyperbolic problem for $u = u(x,t)$:

$$\partial u / \partial t + c \partial u / \partial x = 0, \; x \in R^1 \; and \; t > 0 \tag{4a}$$

$$u(x,0) = u_0(x) \; (initial \; condition), \; x \in R^1 \tag{4b}$$

where $u_0(x)$ is assumed to vanish at infinity. By replacing x with $G[\xi]$, a problem for $\upsilon(\xi, t)$, equivalent to Equation.(4) is obtained, such that

$$\begin{gathered} \partial \upsilon / \partial t + c a(\xi) \partial \upsilon / \partial \xi = 0, \; x \in J \; and \; t > 0 \\ \upsilon(\xi, 0) = \upsilon_0(\xi), \xi \in J \text{ (initial condition)} \\ \upsilon(\xi, t) = 0, \; \xi = \pm L \text{ (boundary condition)} \end{gathered} \tag{5}$$

, where $\upsilon(\xi, t) = u(G[\xi], t)$ and $v_0(\xi) = u_0(G[\xi])$.

Equation (5) can be solved numerically at discrete times, $t = t_n$, using an appropriate finite difference scheme for hyperbolic problems of the first order, such as Friedrichs' scheme or Lax-Wendroff's scheme, on equally spaced mesh points, ξ^j, of width h, over the closed interval, $[-L, L]$. Let v_h denote this solution. Then $v_h(\xi^j, t_n)$ must be a numerical solution to equation (4) at $x^j = G[\xi^j]$, $t = t_n$. An important point is that mapping back from ξ to x is not actually needed for the mesh points inside I_ξ, because of the property of identity mapping of G. The 'shrink-mapped' region J' can be viewed as if it absorbs waves emitted into it.

The extension to problems in n coordinate variables $x_k (k = 1, \ldots n)$ can be made by replacing each x_k with $G[\xi_k]$; this is equivalent to replacing $\partial / \partial x_k$ with $a(\xi_k) \partial / \partial \xi_k$. The proof of convergence has been shown in [5]. for certain different schemes, when used to solve the 'shrink-mapped' version of a general class of hyperbolic systems of the fi;rst order

Application to nonlinear foundation soil

Two dimensional momentum equations of foundation soil is given below

$$\rho \frac{\partial^2 U}{\partial t^2} = \frac{\partial \sigma_x}{\partial x} + \frac{\partial x}{\partial z}, \quad \rho \frac{\partial^2 W}{\partial t^2} = \frac{\partial \tau}{\partial x} + \frac{\partial \sigma_z}{\partial z} \tag{6}$$

, where ρ is density, U and W are horizontal and vertical displacement, and σ_x, σ_z, τ are stress tensor components. Constitutive equations can be given as follows.

$$\frac{\partial \sigma_x}{\partial t} = (\lambda + 2\mu) \frac{\partial u}{\partial x} + \lambda \frac{\partial w}{\partial z}, \quad \frac{\partial \tau}{\partial t} = \mu \left\{ \frac{\partial u}{\partial z} + \frac{\partial w}{\partial x} \right\}, \quad \frac{\partial \sigma_z}{\partial t} = \lambda \frac{\partial u}{\partial x} + (\lambda + 2\mu) \frac{\partial w}{\partial z} \tag{7}$$

, where u and w are horizontal and vertical components of velocities and, λ and μ are instantaneous Lamb's constants. These equations are transformed into first order equations as follows.

$$\frac{\partial \vec{u}}{\partial t} = A_x \frac{\partial \vec{u}}{\partial x} + A_z \frac{\partial \vec{u}}{\partial z} \tag{8}$$

, where $\vec{u} = (u, w, \sigma x, \tau, \sigma_z)^T$, and A_x and A_z are given below

$$A_x = \begin{bmatrix} 0 & 0 & \frac{1}{\rho} & 0 & 0 \\ 0 & 0 & 0 & \frac{1}{\rho} & 0 \\ \lambda+2\mu & 0 & 0 & 0 & 0 \\ 0 & \mu & 0 & 0 & 0 \\ \lambda & 0 & 0 & 0 & 0 \end{bmatrix}, \quad A_z = \begin{bmatrix} 0 & 0 & \frac{1}{\rho} & 0 & 0 \\ 0 & 0 & 0 & 0 & \frac{1}{\rho} \\ 0 & \lambda & 0 & 0 & 0 \\ \mu & 0 & 0 & 0 & 0 \\ 0 & \lambda+2\mu & 0 & 0 & 0 \end{bmatrix} \tag{9}$$

The following shrink mapping is introduced

$$x = G(x') \equiv \int_0^{x'} \frac{dx'}{a(x')}, \quad \left| x' \right| \le Lx$$

$$z = H(z') \equiv \int_0^{z'} \frac{dz'}{b(z')}, \quad -Lz \le z' \le 0 \tag{10}$$

, where

$$a(x') = 1, \left| x' \right| \le \ell x \text{ (isometric)}$$

$$a(x') = 1 - 1/2(\ell x - \left| x' \right|)^2, \ell x < \left| x' \right| \le 1/2(Lx + \ell x) \text{ (shrink)}$$

$$a(x') = 1/2(Lx - \left| x' \right|)^2, 1/2(Lx + \ell x) < \left| x' \right| \le Lx \text{ (shrink)} \tag{11}$$

$$b(z') = 1, \left| z' \right| \le \ell z \text{ (isometric)}$$

$$b(z') = 1 - 1/2(\ell z - \left| z' \right|)^2, \ell z < \left| z' \right| \le 1/2(Lz + \ell z) \text{ (shrink)}$$

$$b(z') = 1/2(Lz - \left| z' \right|)^2, 1/2(Lz + \ell z) < \left| z' \right| \le Lz \text{ (shrink)} \tag{12}$$

The equations of motion are expressed as follows

$$\frac{\partial \vec{v}'}{\partial t} = Bx \frac{\partial \vec{v}'}{\partial x'} + Bz \frac{\partial \vec{v}'}{\partial z'} \tag{13}$$

, where

$$\vec{v}' = (u', w', \sigma_x', \tau', \sigma_z')^t, Bx = a(x')Ax(G(x'), H(z')), Bz = b(x')Az(G(x'), H(z'))$$

and $u', w', \sigma_x', \tau', \sigma_z'$ are velocities and stress tensor components in transformed coordinates. Equation 13 is solved with a product-type formula of a one-dimensional Lax-Wendroff scheme on uniform mesh of finite differences. The difference solution, $\vec{v}'$ at time t_{n+1} is obtained from $\vec{v}'$ at t_n by:

$$\vec{v}' = L_x L_z \vec{v}' \tag{14}$$

, where L_x and L_z, respectively, are the two step Lax-Wendoroff difference operators to solve the one dimensional problem $\partial v / \partial t = B_x(x) \partial v / \partial x$ and $\partial v / \partial t = B_z(z) \partial v / \partial z$ .The following is the explicit formula for integration:

$$\begin{Bmatrix} u \\ w \\ \sigma_x \\ \tau \\ \sigma_z \end{Bmatrix}_{i-\frac{1}{2},k}^{n+\frac{1}{2}} = \frac{1}{2} \left(\begin{Bmatrix} u \\ w \\ \sigma_x \\ \tau \\ \sigma_z \end{Bmatrix}_{i,k}^{n} + \begin{Bmatrix} u \\ w \\ \sigma_x \\ \tau \\ \sigma_z \end{Bmatrix}_{i-1,k}^{n} \right) + \frac{\Delta t a (i - \frac{1}{2})}{2h} \left[Bx \right]_{i-\frac{1}{2},k}^{n} \left(\begin{Bmatrix} u \\ w \\ \sigma_x \\ \tau \\ \sigma_z \end{Bmatrix}_{i,k}^{n} - \begin{Bmatrix} u \\ w \\ \sigma_x \\ \tau \\ \sigma_z \end{Bmatrix}_{i-1,k}^{n} \right) \tag{15}$$

$$\begin{Bmatrix} u \\ w \\ \sigma_x \\ \tau \\ \sigma_z \end{Bmatrix}_{i,k}^{n+1} = \begin{Bmatrix} u \\ w \\ \sigma_x \\ \tau \\ \sigma_z \end{Bmatrix}_{i,k}^{n} + \frac{\Delta t a(\dot{x})}{h} \left[Bx \right]_{i,k}^{n+\frac{1}{2}} \left(\begin{Bmatrix} u \\ w \\ \sigma_x \\ \tau \\ \sigma_z \end{Bmatrix}_{i+\frac{1}{2},k}^{n+\frac{1}{2}} - \begin{Bmatrix} u \\ w \\ \sigma_x \\ \tau \\ \sigma_z \end{Bmatrix}_{i-\frac{1}{2},k}^{n+\frac{1}{2}} \right) \tag{16}$$

$$\begin{Bmatrix} u \\ w \\ \sigma_x \\ \tau \\ \sigma_z \end{Bmatrix}_{i,k-\frac{1}{2}}^{n+\frac{1}{2}} = \frac{1}{2} \left(\begin{Bmatrix} u \\ w \\ \sigma_x \\ \tau \\ \sigma_z \end{Bmatrix}_{i,k}^{n} + \begin{Bmatrix} u \\ w \\ \sigma_x \\ \tau \\ \sigma_z \end{Bmatrix}_{i,k-1}^{n} \right) - \frac{\Delta t b(k-\frac{1}{2})}{2h} \left[Bz \right]_{i,k-\frac{1}{2}}^{n} \left(\begin{Bmatrix} u \\ w \\ \sigma_x \\ \tau \\ \sigma_z \end{Bmatrix}_{i,k}^{n} - \begin{Bmatrix} u \\ w \\ \sigma_x \\ \tau \\ \sigma_z \end{Bmatrix}_{i,k-1}^{n} \right) \tag{17}$$

$$\begin{Bmatrix} u \\ w \\ \sigma_x \\ \tau \\ \sigma_z \end{Bmatrix}_{i,k}^{n+1} = \begin{Bmatrix} u \\ w \\ \sigma_x \\ \tau \\ \sigma_z \end{Bmatrix}_{i,k}^{n} - \frac{\Delta t b(k)}{h} \left[Bz \right]_{i,k}^{n+\frac{1}{2}} \left(\begin{Bmatrix} u \\ w \\ \sigma_x \\ \tau \\ \sigma_z \end{Bmatrix}_{i,k+\frac{1}{2}}^{n+\frac{1}{2}} - \begin{Bmatrix} u \\ w \\ \sigma_x \\ \tau \\ \sigma_z \end{Bmatrix}_{i,k-\frac{1}{2}}^{n+\frac{1}{2}} \right) \tag{18}$$

, where Δt , h are time increment and mesh width, respectively, and super scripts and sub scripts indicate time points and grid points, respectively.

Vertically propagating incident waves are solved as in the following. It is assumed that Soil is linear beyond k_0 meshes from the surfaces, and that the response is given by superposition of the incident wave propagating upward and reflected wave going downward. The incident wave is assumed to be uniform in horizontal direction. Variables with subscript I correspond to incident wave. Variables computed are total for $k<k_0$, while variables corresponding to downward wave only are calculated for $k \geq k_0$. The resulting finite difference equations for $k = k_0 - \frac{1}{2}$ are given as:

$$v_{i,k-\frac{1}{2}}^{n+\frac{1}{2}} = \frac{1}{2}(v_{i,k}^{n} + v_{i,k-1}^{n} + v_{I,k0}^{n}) - \frac{b(k-\frac{1}{2})\Delta t}{2h} \frac{1}{\rho_{i,k-\frac{1}{2}}} (\tau_{i,k}^{n} - \tau_{i,k-1}^{n} + \tau_{I,k0}^{n}) \tag{19}$$

$$w_{i,k-\frac{1}{2}}^{n+\frac{1}{2}} = \frac{1}{2}(w_{i,k}^{n} + w_{i,k-1}^{n} + w_{I,k0}^{n}) - \frac{b(k-\frac{1}{2})\Delta t}{2h} \frac{1}{\rho_{i,k-\frac{1}{2}}} (\sigma_{i,k}^{n} - \sigma_{i,k-1}^{n} + \sigma_{I,k0}^{n}) \tag{20}$$

$$\sigma_{x}{}_{i,k-\frac{1}{2}}^{n+\frac{1}{2}} = \frac{1}{2}(\sigma_{i,k}^{n} + \sigma_{i,k-1}^{n} + \sigma_{I,k0}^{n}) - \frac{b(k-\frac{1}{2})\Delta t}{2h} \lambda_{i,k-\frac{1}{2}}^{n} (w_{i,k}^{n} - w_{i,k-1}^{n} + w_{I,k0}^{n}) \tag{21}$$

$$\tau_{i,k-\frac{1}{2}}^{n+\frac{1}{2}} = \frac{1}{2}(\tau_{i,k}^{n} + \tau_{i,k-1}^{n} + \tau_{I,k0}^{n}) - \frac{b(k-\frac{1}{2})\Delta t}{2h} \mu_{i,k-\frac{1}{2}}^{n} (v_{i,k}^{n} - v_{i,k-1}^{n} + v_{I,k0}^{n}) \tag{22}$$

$$\sigma_{z}{}_{i,k-\frac{1}{2}}^{n+\frac{1}{2}} = \frac{1}{2}(\sigma z_{i,k}^{n} + \sigma z_{i,k-1}^{n} + \sigma z_{I,k0}^{n}) - \frac{b(k-\frac{1}{2})\Delta t}{2h} (\lambda + 2\mu)_{i,k-\frac{1}{2}}^{n} (w_{i,k}^{n} - w_{i,k-1}^{n} + w_{I,k0}^{n}) \tag{23}$$

and for $k=k_0$

$$\upsilon_{i,k}^{n+1}=\upsilon_{i,k}^{n}-\frac{b_{(k)}\Delta t}{h}\frac{1}{\rho_{i,k}}\left(\tau^{n+\frac{1}{2}}_{i,k+\frac{1}{2}}+\tau^{n+\frac{1}{2}}_{I,k0+\frac{1}{2}}-\tau^{n+\frac{1}{2}}_{k-\frac{1}{2}}\right) \tag{24}$$

$$w_{i,k}^{n+1}=w_{i,k}^{n}-\frac{b_{(k)}\Delta t}{h}\frac{1}{\rho_{i,k}}\left(\sigma_{z_{i,k+\frac{1}{2}}}^{n+\frac{1}{2}}+\sigma_{z_{I,k0+\frac{1}{2}}}^{n+\frac{1}{2}}-\sigma_{z_{k-\frac{1}{2}}}^{n+\frac{1}{2}}\right) \tag{25}$$

$$\sigma x_{i,k}^{n+1}=\sigma_{xi,k}^{\ n}-\frac{b_{(k)}\Delta t}{h}\lambda_{i,k}^{n+\frac{1}{2}}\left(w^{n+\frac{1}{2}}_{i,k+\frac{1}{2}}+w^{n+\frac{1}{2}}_{I,k0+\frac{1}{2}}-w^{n+\frac{1}{2}}_{k-\frac{1}{2}}\right) \tag{26}$$

$$\tau_{i,k}^{n+1}=\tau_{i,k}^{n}-\frac{b_{(k)}\Delta t}{h}\lambda_{i,k}^{n+\frac{1}{2}}\left(\upsilon^{n+\frac{1}{2}}_{i,k+\frac{1}{2}}+\upsilon^{n+\frac{1}{2}}_{I,k0+\frac{1}{2}}-\upsilon^{n+\frac{1}{2}}_{k-\frac{1}{2}}\right) \tag{27}$$

$$\sigma z_{i,k}^{n+1}=\sigma_{z_{i,k}}^{n}-\frac{b_{(k)}\Delta t}{h}(\lambda+\upsilon)_{i,k}^{n+\frac{1}{2}}\left(w^{n+\frac{1}{2}}_{i,k+\frac{1}{2}}+w^{n+\frac{1}{2}}_{I,k0+\frac{1}{2}}-w^{n+\frac{1}{2}}_{k-\frac{1}{2}}\right) \tag{28}$$

Hybrid Finite Element and finite difference scheme

FEM is suited for dealing with the irregularities of geometry and heterogeneity of materials. Dynamic soil-structure problem may be treated well by hybrid method, in which structure and near by portion of soil is analyzed by FEM, while finite difference method is applied to far field. As a specimen problem, two-dimensional dam-foundation soil reservoir system illustrated in Fig.1 is considered. Zone1 is the near field zone, which covers the dam and its near-by portion of water and foundation soil. Zone 2 covers the far field portion of foundation soil and zone 3 the far field portion of reservoir water. Zone 1 and zone 2, as well as zone 1 and zone 3, overlap by one mesh width. In zone 3, the shrink-mapped hyperbolic system equivalent to the wave equation for velocity potential is solved using finite differences. The system is given by:

$$\frac{\partial}{\partial t}\begin{Bmatrix}\dot{\phi}\\ \xi\\ \varsigma\end{Bmatrix}=a(x)\begin{bmatrix}0 & C_0^{\ 2} & 0\\ 1 & 0 & 0\\ 0 & 0 & 0\end{bmatrix}\begin{Bmatrix}\dot{\phi}\\ \xi\\ \varsigma\end{Bmatrix}+\begin{bmatrix}0 & 0 & C_0^{\ 2}\\ 0 & 0 & 0\\ 1 & 0 & 0\end{bmatrix}\begin{Bmatrix}\dot{\phi}\\ \xi\\ \varsigma\end{Bmatrix} \tag{29}$$

, where $\dot{\phi}=\partial\phi/\partial t$, $\xi=\partial\phi/\partial x$,and $\varsigma=\partial\phi/\partial y$.

Time integration is made in the same way as in Zone 2. In zone 1,finite element modeling using isoparametric elements is applied. Crack generation and extension is analyzed as follows.

(1) Crack is generated at upstream or downstream face of the dam, if the primary principal stress at a Gauss point in a element along the upstream, or downstream face exceeds the tensile strength of concrete. The boundary between the elements nearest to the Gauss point is separated.

(2) When a crack extends, dependent energy release should exceed the energy required for extension of crack.

(3) Opening and closure of a crack are simulated by inserting a joint element automatically in the crack. The joint element is 6 nodes element using 3 points Newton Cotes integration. The stiffness normal to or tangential to the crack changes according to the crack opening displacement at each integration point. If the opening displacement is within a threshold value, the tangential and normal stiffness are SN1, and SS2, respectively, while the opening displacement is greater than the threshold value, the stiffness are SN2,and SS2, where SN1>>SN2 and SS1>>SS2.

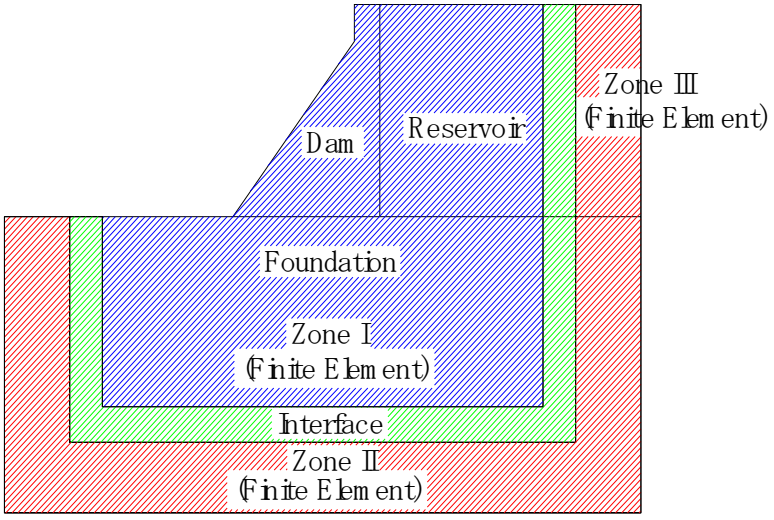

Fig.1 Hybrid Model

NUMERICAL EXAMPLE 1

Two-dimensional problems of semi-infinite foundation soil are solved with the proposed method. The model in the transformed domain is shown in Fig.2 and 3. IEND and KEND are total numbers of meshes in horizontal and vertical directions. IABSL, IABSR, and KABSB are numbers of meshes for shrink mapping. In these examples, IABSL, IABSR, and KABSB are fixed to be 10.

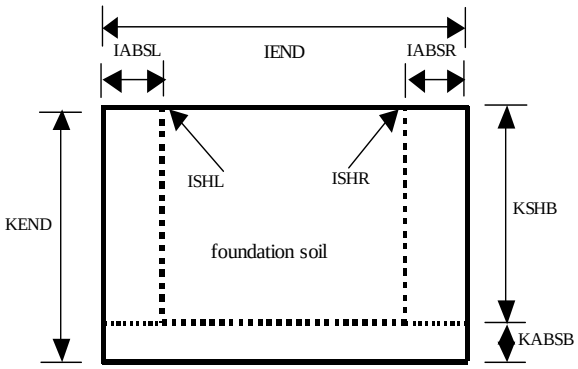

Fig.2 Ground model in transformed infinite domain

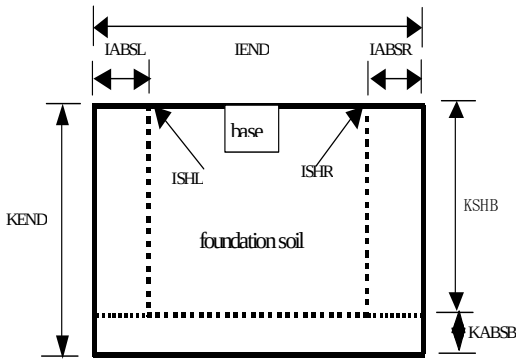

Fig.3 Model in transformed domain

At first, linear problems are solved. Material properties of soil are assume to be ρ=1, λ=15000, μ=10000. The mesh width $h=1$ and time increment Δt= 0.002 are adopted. Figure 4 shows the equivalent stiffness for a uniform harmonic loadings obtained by the proposed method and the theoretical values using the method of Fourier transforms, given in Hanada[6]. Good agreements are obtained between theoretical and calculated results using small models (IEND=31,KEND=21,KSHB=IABSL=IABSR=10). Then, transient responses of foundation soil to surface loadings $f(t)$, i.e. Lamb's problem, are calculated by proposed method, and compared with theoretical values. Ricker wavelet $f(t)=\alpha(1-2\alpha^2t^2)e^{-\alpha^2t^2}/2\sqrt{\pi}$, $(\alpha=2\pi)$ is applied horizontally on the surface of the ground, and out of plane velocity of the ground is compared with

theoretical results in Fig.5. Good agreement is obtained. Fig.6 and Fig7 shows the responses to vertical Ricker wavelet on the ground surface calculated by proposed method and FEM with conventional boundary conditions, i.e., displacement normal to the boundary is fixed, with different mesh extent. The results of proposed method are independent of the mesh extent, while the results of FEM with conventional boundary condition depends on the extent of meshes due to the existence of reflective waves.

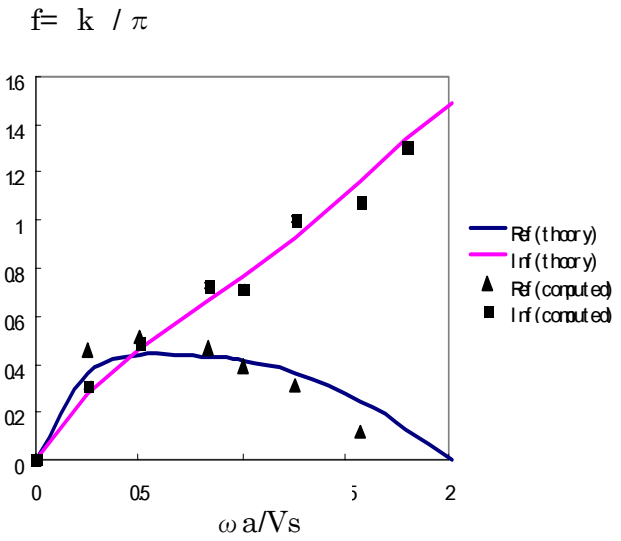

Fig. 4-: Equivalent stiffness of semi -infinite body for uniform vertical loading of surface

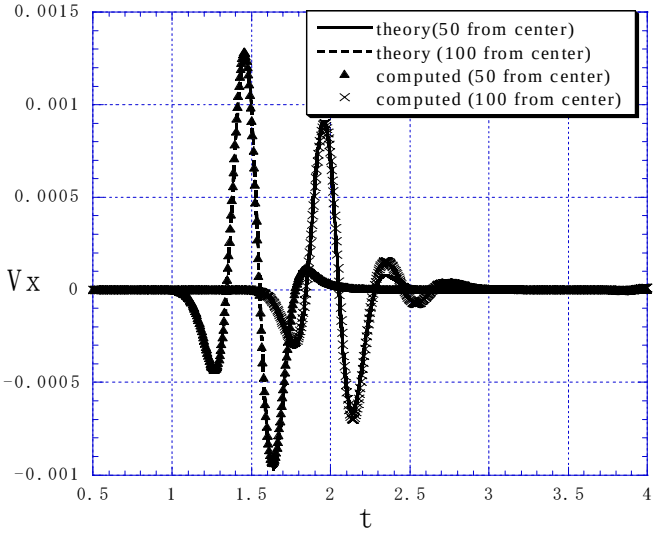

Fig. 5 Comparison of the results of proposed and Lamb's theory. (horizontal velocity response mesh 231*121)

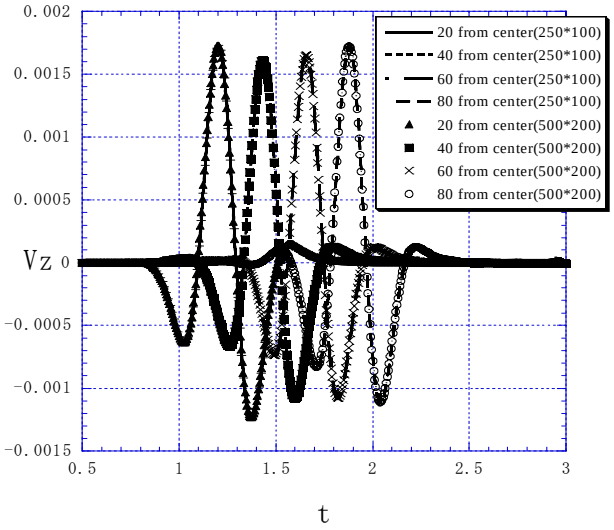

Fig.6 Comparison of the results of proposed method with different mesh. (Vertical velocity response)

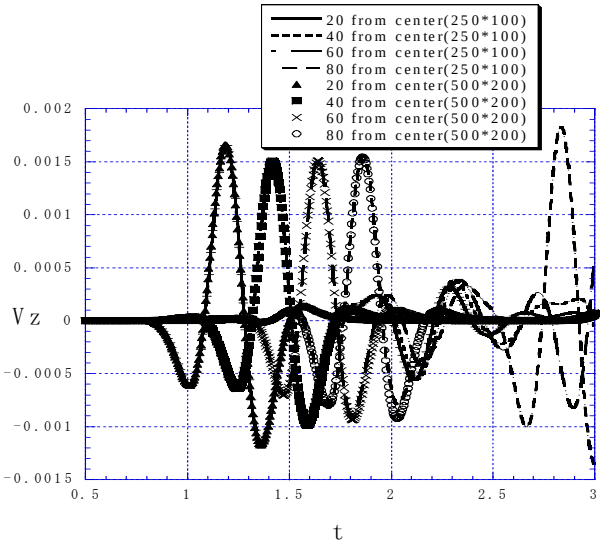

Fig.7 Comparison of the results of FEM with different mesh. (Vertical velocity response)

Next, vertically propagating incident wave is applied to the nonlinear ground. The horizontal velocity of incident wave is given by $0.5(1-\cos(2\pi\ t/T_0))$, where the period $T_0=0.2$, and the duration time is equal to the period. The relationship between shear stress and shear strain is assumed to be $\tau=\mu_0(1+\mu_1\gamma^2+\mu_2\gamma^4)\gamma$, where γ is shear strain. The bulk modulus and density of soil is set to be the same as these of the linear models. In addition, 7×7meshes are used to represent base (see Fig. 3), where the density and stiffness are assumed to be twice as much as those of the soil. The responses of the linear and

nonlinear models ($\mu_1 = \mu_2 = 10000$) with different mesh are shown in Fig. 8 and 9. Nonlinear response calculated with small model (31×31) or large model (231×131) coincide with each other.

Linear and non-linear responses of base-soil mode1 shown in Fig.3 are computed again Wen's general nonlinear hysteretic model is adopted for nonlinear constitutive model of soil, with $\alpha = \beta = 100$, and $n = 1$ Wen[7]. Non-dimensional values of mass density, Lame's constants are, $\rho_0 = 1,$. $\lambda_0 = 10000,$ and $\mu_0 = 10000$, respectively, Fig.10 shows non-linear stress-strain relationships of soil subjected to vertically propagating half cycle of sinusoidal shear wave with velocity amplitude of 1.0 and period of 1.0. The incident wave is applied 20 meshes below the surface. The responses of the base model of Fig.3 to the incident wave are computed with different meshes (IEND=51 and kend=70, IEND=231 and KEND=121, and IEND=431 and KEND=221), and results with linear soil model are shown in Fig.11. The base is 6 meshes wide and 4 meshes deep, and assumed to be linear with the density and the stiffness 6 times as much as those of linear soil. The computed responses are not dependent on the extent of meshes. Fig.12 shows the results with non-linear soil model. The amplitudes of the responses are smaller, and phase delays are larger than the corresponding results with linear soil. Again, the results are virtually the same, irrespective of extent of meshes. The responses of the base embedded in nonlinear soil of 20 meshes wide and 20 meshes deep, are computed, and shown in Fig.13. The non-linear soil is surrounded by linear soil of different extent of meshes (IEND=231 and KEND=121, and IEND=431 and KEND=221). The responses are equal to neither those of linear model nor those of nonlinear model. This implies that analytical results with non-linearity restricted to nearby portion of structures may be different from full nonlinear model when extensive foundation soils become nonlinear.

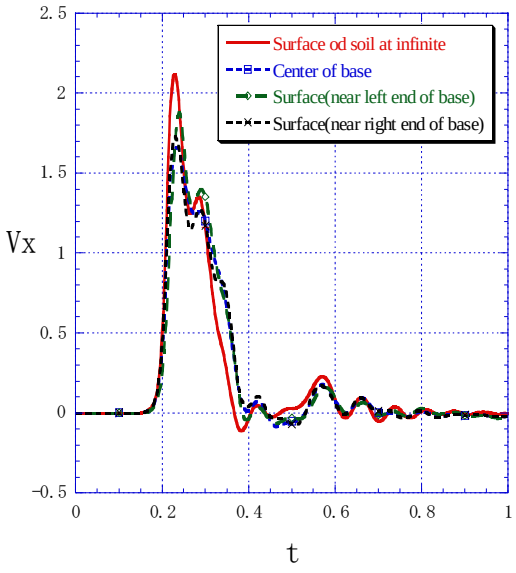

Fig. 8: Response of horizontal velocity to incident wave(nonlinear model,meshes31*31)

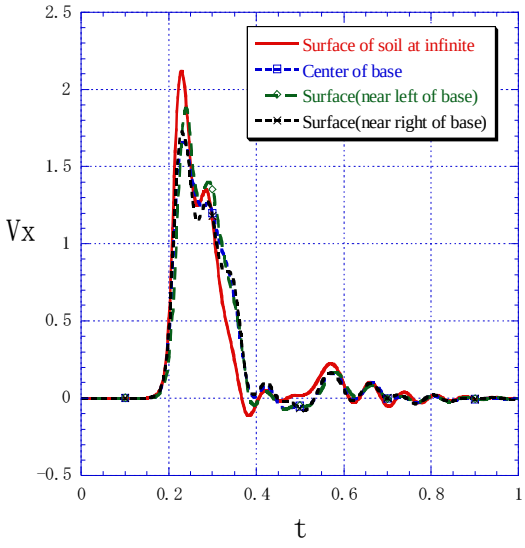

Fig. 9: Response of horizontal velocity to incident wave(nonlinear model, meshes231*131)

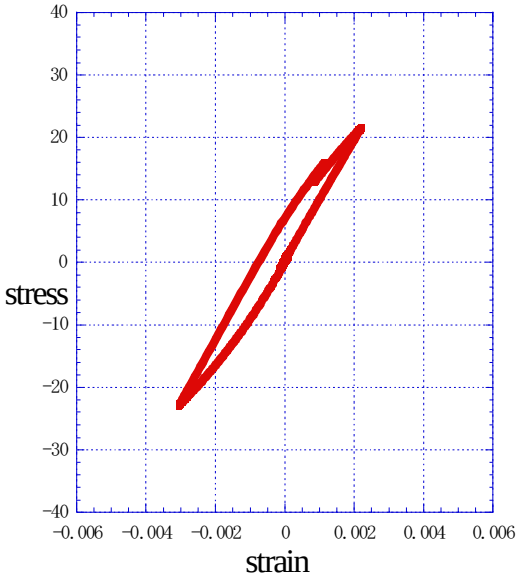

Fig.10 Shear stress-strain relationship. (nonlinear model, mesh51*70)

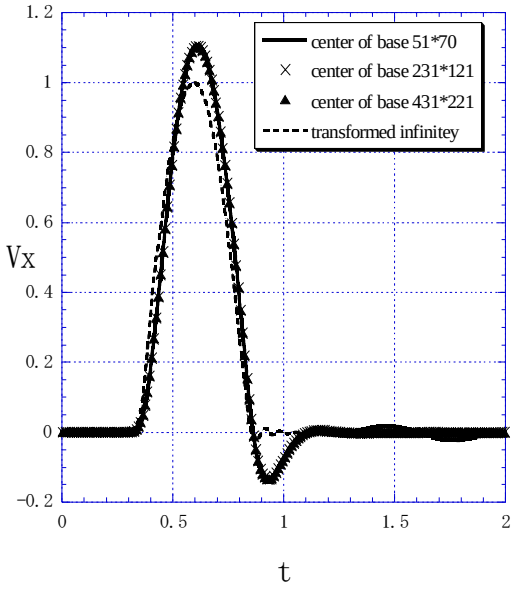

Fig. 11 Response of horizontal velocity to incident wave (linear model)

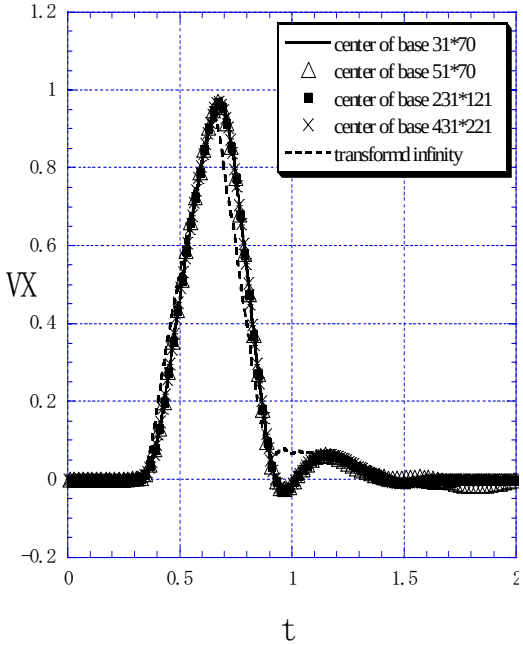

Fig.12 Response of horizontal velocity to incident wave. (nonlinear model)

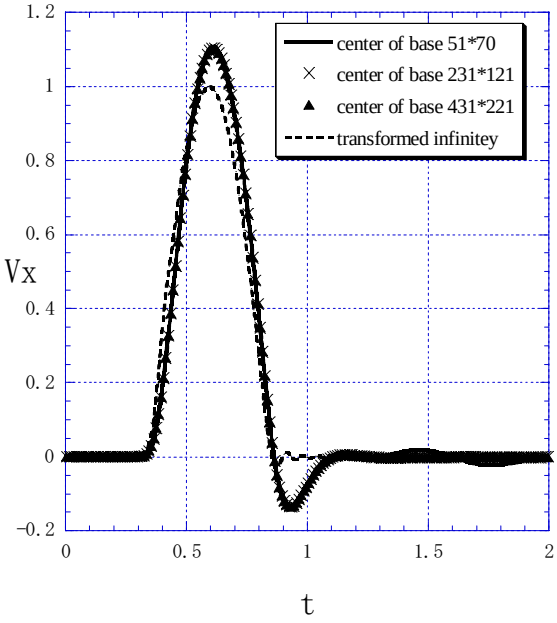

Fig.13 Response of horizontal velocity to incident wave. (linear and nonlinear model)

Numerical example 2

The earthquake responses of a dam-foundation rock-reservoir water system are computed by hybrid finite element-shrink mapped finite difference method. The dam is 100 m high, and the mesh for FEM is shown in Fig.17. Some of material properties are shown in Table 1. Tensile strength of dam concrete is assumed to be $2.0\times10^{6}\,\mathrm{N/m^2}$, and fracture energy 3000N/m.

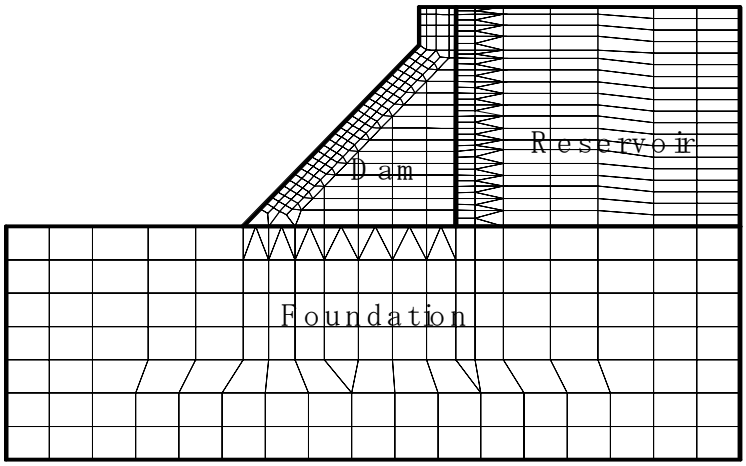

Fig.14. Mesh of Dam-Reservoir Water-Foundation Rock System for FEM

Table.1 Material Properties

	Density (kg/m^3)	Young's Modulus (N/m^2)	Poisson's Ratio	Lame's Constant (N/m^2)	Lame's Constant (N/m^2)	P Wave velocity (m/s)
rock	2.2×10^{3}	2.0×10^{10}	0.3	1.154×10^{10}	7.692×10^{9}	3498
concrete	2.4×10^{3}	3.0×10^{10}	0.2	8.33×10^{9}	1.25×10^{10}	3726

The responses of the system to 1995 Kobe earthquake shown in Fig.15 are computed. The acceleration responses of dam crest are given in Fig.16 and Fig.17. It is shown in Fig.16 that the response of the dam with reservoir water full is greater, and dominant period is longer compared to those with empty reservoir. Fig.17 shows the difference due to the consideration of crack. The response becomes larger and impulsive accelerations are generated due to opening and closure of cracks

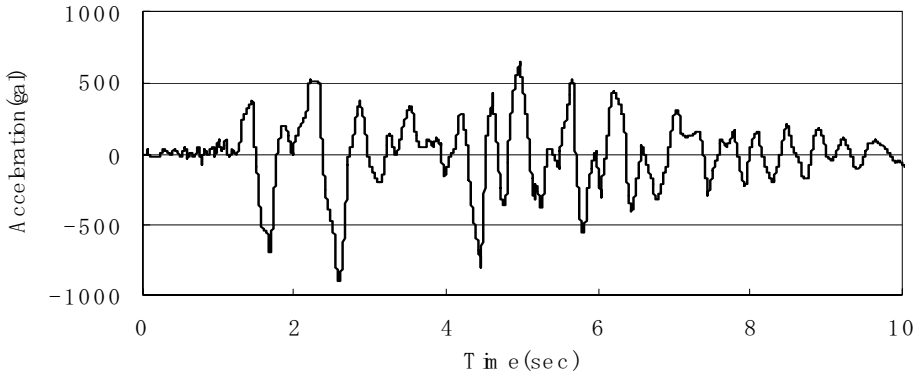

Fig.15 Earthquake Wave (1995 Kobe)

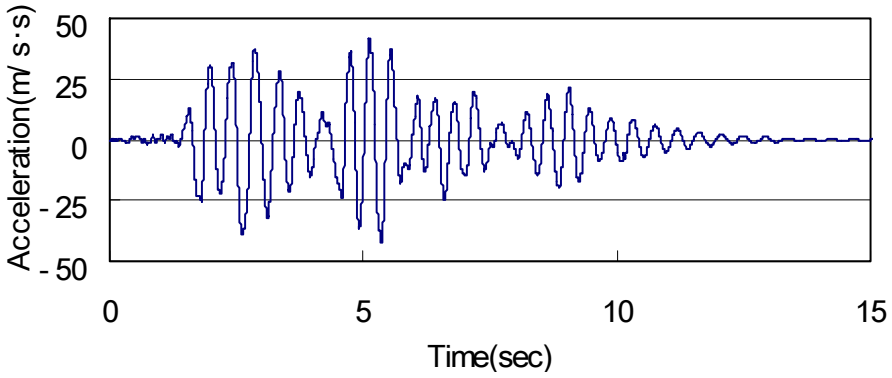

(a)With Reservoir Water

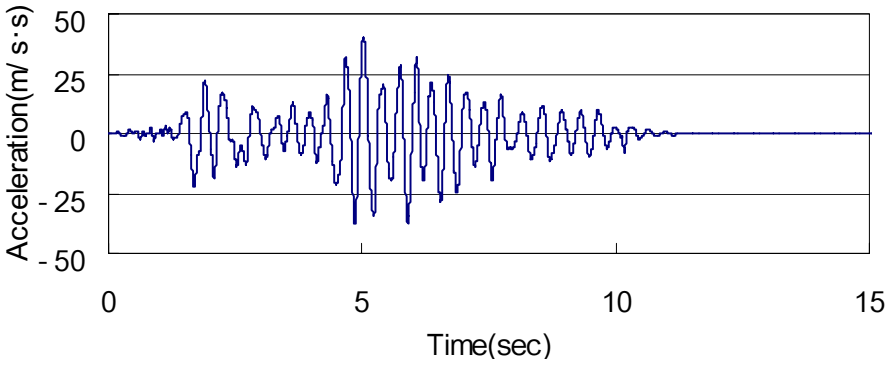

(b) Without Reservoir Water

Fig.16 Acceleration Response of Dam Crest (with and without Reservoir Water)

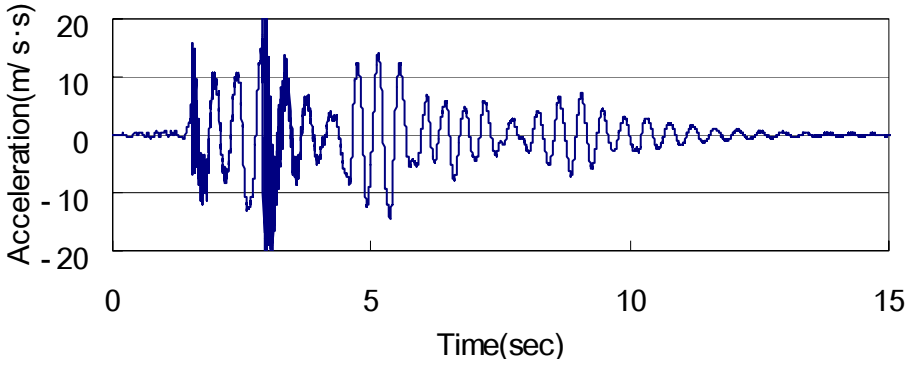

(a)With Crack

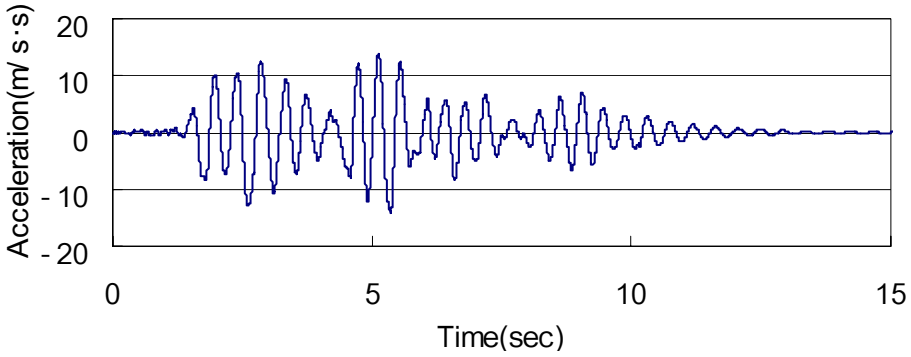

(b)Without Crack

Fig.17 Acceleration Response of Dam Crest (with and without Consideration of Crack)

CONCLUSIONS

A special finite element method is developed for the non-linear analysis of semi-infinite foundation soil. Computed results are compared with theoretical ones for linear problem and, good agreements are obtained. By numerical examples using small meshes and extensive meshes for nonlinear problems, it is demonstrated that semi-infinite non-linear soil can be effectively treated with small number of meshes. The dynamic response analysis of dam-reservoir-foundation system considering crack generation is effectively conducted by combining FEM with the proposed method.

ACKNOWLEDGMENTS

This research was conducted as a part of the Academically Promoted Frontier Research Program on "Sustainable City Based on Environmental Preservation and Disaster Prevention" at Nihon University, College of Science and Technology under a Grant from the Ministry of Education, Science and Sports, Japan.

REFERENCES

1. Wolf, J. P., “Soil-Structure-Interaction Analysis in Time Domain”, Prentice-Hall. 1988.
2. Shiojiri H., Nakagawa T. T., “Soil-Structure-Interaction Numerical Analysis and Modeling” The Chapter 6 Earthquake Response of Dams, E&FN SPON., Press, pp.202-230, 1994.
3. Shiojiri H., “Earthquake response of structure considering hydrodynamic and foundation interaction effects” Central Research Institute of Electric Power Industry. pp.7-29, Sep 1986 (in Japanese).
4. Watanabe H., Cao Z., “Upstream Boundary of Reservoir in Dynamic Analysis”, Journal of Engineering Mechanics, ASCE, Vol.124, No.4, Apr 1998.
5. Nakagawa T. T, ”The near-field difference solution for wave propagation problems in infinite media.” studies in Mathematics and its Applications, Kinokuniya/North-Holland Publishing Co., 18, 1986, 561.
6. Hanada K., “ Analysis on Dynamic behaviors of Soil-Structure Systems.” Central Research Institute of Electric Power Industry. Technical Number: 74546, May 1975.
7. Wen Y. K., “Method for Random Vibration of Hysteretic Systems”, Journal of The Engineering Mechanics Division. pp. 249-263, 1976.